Development of Selective Fluorescence Neurosensor for Neurotransmitter Monitoring in Live Cells

---

A Thesis

Presented to

the Faculty of Graduate School

at the University of Missouri-Columbia

In Partial Fulfillment

of the Requirements for Degree

Master of Science

By

Ramin Tajali

Dr. Timothy E. Glass, Thesis Supervisor

DECEMBER 2022

The undersigned, appointed by the dean of the Graduate School, have examined the dissertation entitled

Development of Selective Fluorescence Neurosensor for Neurotransmitter Monitoring in Live Cells

presented by Ramin Tajali,

a candidate for the degree of Master of Science,

and hereby certify that, in their opinion, it is worthy of acceptance.

_____

Professor Timothy E. Glass, Thesis Supervisor

_____

Professor Kent S. Gates, Committee Member

_____

Professor C. Michael Greenlief, Committee Member

_____

Professor Ilker Ozden, Committee Member

Acknowledgments

First, I would like to express my deepest gratitude to my M.S. supervisor, Dr. Timothy E. Glass. This endeavor would not have been possible without his support, guidance, encouragement, and patience. I would also like to thank my committee members for their efforts and contributions to this work: Dr. Kent S. Gates, Dr. C. Michael Greenlief, and Dr. Ilker Ozden.

Finally, many thanks also go to the current and past members from the Glass group, Anusha Bade, Mandana Taheri, John Himmelberg, Ramesh Bypaneni, Faith Aynekulu, Glenn Gilyot, Peeyush Yadav, and Alyssa Weyl. They provided an amazing work environment during my M.S. study. I would like to thank all faculty, staff members, graduate students in Chemistry department.

Table of Contents

Acknowledgments……....ii

List of Schemes…….v

List of Figures……...…vi

List of Tables……...……..viii

Abstract…….....ix

Chapter 1: Fluorescence…….……...…...……1

1.1: Introduction to Fluorescence……1

1.2. Fluorescence Quantum Yield and Stokes Shift……2

1.3. Fluorescence Signaling Mechanisms……...……...……4

1.3.1. Photoinduced Electron Transfer (PET) ……4

1.3.2. Fluorescence Resonance Energy Transfer (FRET) ……..……5

1.3.3. Internal Charge Transfer (ICT) ……6

1.4. Fluorophore……..7

1.5. Fluorescence Quenching Mechanisms…….8

1.6. Conclusion……9

Chapter 2: Neurotransmitters…….……..10

2.1. Introduction to Neurotransmitter……10

2.1.1. Glutamate……...…….……13

2.1.2. Gamma-Aminobutyric Acid (GABA) ……...…….……13

2.1.3. Glycine……....…14

2.2. Boronic Acid Fluorescence Sensor……...……..14

2.2.1. Overview……..14

2.2.2. Boronic Acid Binding Constant……...……15

2.2.3. Boronic Acid Fluorescence Sensors……...……16

2.3. Conclusion……..17

Chapter 3: Experimental Approach toward Synthesis of Neurosensor1…….……...……19

3.1. Background…….....……...….19

3.2. Goal…….……20

3.3. Synthesis of Neurosensor1…….…….21

3.3.1. First Synthesis Approach…….……21

3.3.2. Alternative Synthesis Approach……..…28

3.3.3. Future Work……...……..30

Supplemental Information……...……...……31

References……...……41

List of Schemes

Scheme 3.1. Synthesis of 7-diethylamino 4-hydroxycoumarin……...……21

Scheme 3.2. Synthesis of Naphthalene diboronic acid……22

Scheme 3.3. Synthesis of 7-diethylamino 4-arylcoumarin……..…23

Scheme 3.4. Synthesis of designed fluorescence sensor…….…..……23

Scheme 3.5. Vilsmeier-Haack reaction……24

Scheme 3.6. Synthesis of 7-diethylamino 4-bromocoumarin……..….28

Scheme 3.7. Synthesis of 7-diethylamino 4-diboronic ester coumarin……...……29

Scheme 3.8. Synthesis of 7-diethylamino 4-diboronic ester coumarin……...……29

Scheme 3.9. Synthesis of compound 5……..……..30

Scheme 3.10. Synthesis of neurosensor1…….……30

List of Figures

Figure 1.1. Jablonski diagram and energy levels……...……2

Figure 1.2. Stokes shift in fluorescence…….3

Figure 1.3. Molecular orbital energy diagram illustrating PET mechanism……..4

Figure 1.4. A model of PET sensor design (A) analyte-free sensor, (B) analyte-bound…..…..5

Figure 1.5. Donor absorption and acceptor emission spectra of an ideal donor-acceptor pair (a). Jablonski diagram illustrating the FRET process (b) …….6

Figure 1.6. N-butyl-4,5-di[(pyridin-2-ylmethyl) amino]-1,8-naphthalimide ICT sensor for Cu (II) sensing…….……7

Figure 2.1. Glutamate function in the synaptic cleft……12

Figure 2.2. Binding mechanism between phenylboronic acid and a diol……...……15

Figure 2.3. Overall binding constant process (K_{eq}) ……...…..16

Figure 2.4. anthrylboronic acids probes for saccharide sensing……..……16

Figure 2.5. A FRET-on based sensor for catecholamine sensing……17

Figure 3.1. Neurosensor 521 and 560……..19

Figure 3.2. Designed fluorescence Neurosensor1 for the detection of gamma amino acids...20

Figure 3.3. The structure of cross-coupling reaction product..……24

Figure 3.4. Binding constants calculated through fluorescence (A) and UV-Vis (B) titrations of compound 3 with glutamate at pH=5……..25

Figure 3.5. Binding constants calculated through fluorescence (A) and UV-Vis (B) titrations of compound 3 with glycine at pH=5.0…….……..25

Figure 3.6. Binding constants calculated through fluorescence (A) and UV-Vis (B) titrations of compound 3 with glycine at pH=7.4…….……..26

Figure 3.7. Binding constants calculated through fluorescence (A) and UV-Vis (B) titrations of compound 3 with GABA at pH=5…….……..26

Figure 3.8. Binding constants calculated through fluorescence titration of compound 3 with glutamate at pH=7.4……...…….27

Figure 3.9. Binding constants calculated through fluorescence titration of compound 3 with GABA at pH=7.4……27

Figure 3.10. Chemical structure of naphthalene diboronic acid…….……..…28

List of Tables

Table 1.1. Most common fluorophores along with their structures and colors……..…..8

Table 2.1. Neurotransmitters along with their structures and biological functions…..……10

Abstract

In the central nervous system, neurotransmitters are responsible for transferring signals from pre-synaptic vesicles to post-synaptic receptors. The most abundant amino acid in brain, glutamate, is a primary excitatory neurotransmitter which plays a major role in regulating many functions in human body such as memory, learning, and long-term depression. Fluorescence approaches as a noninvasive tool provides high spatial resolution in compared with other conventional methods for neurotransmitter detection. Over the last few years, various optical probes have been reported for neurotransmitters sensing, however, they usually suffer from lack of selectivity.

In this work, we plan to develop a turn on fluorescence sensor based on coumarin-3-aldehyde scaffold to selectively recognize gamma-amino acids neurotransmitters like glutamate and GABA in live cells. This neurosensor binds to the analyte through formation an iminium ion and a boronate ester. In this sensor, the distance between aldehyde functional group and boronic acid group can only fit larger gamma-amino acids over other alpha-amino acids.

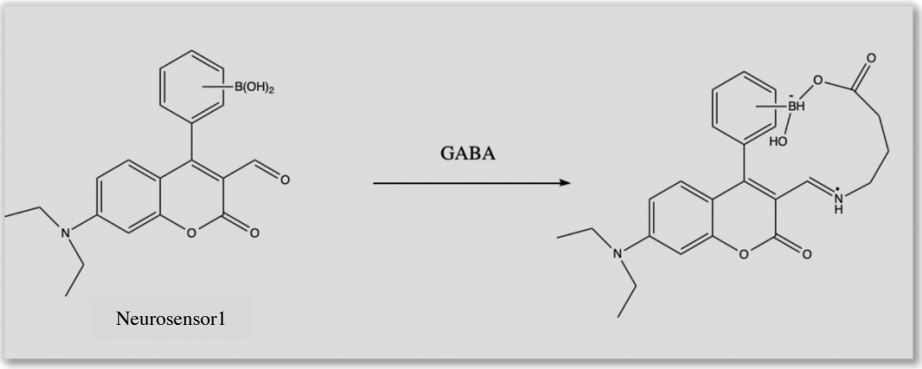

Chapter 1: Fluorescence

1.1 Introduction to Fluorescence

Luminescence is a phenomenon that occurs when a compound in excited state emits light with a certain wavelength. Luminescence is generally categorized into fluorescence and phosphorescence depending on the different arrangement of electrons in the excited state.

The Jablonski diagram shows the different electronic states of a molecule and are widely used to illustrate various type of absorption and emission processes. This diagram is named after Professor Alexander Jablonski who was a pioneer in fluorescence spectroscopy. In a typical Jablonski diagram (figure1.1), the singlet ground state, first and second single excited state are represented by S_0, S_1, and S_2 respectively.[1] The first transition in this diagram is the absorbance of light by the molecule of interest. Once an electron is excited, there are a couple of ways to release this absorbed energy and return to ground electronic state. This energy can be released thorough vibrational relaxations which are shown by yellow curved arrows in diagram. This is a non-radiative and fast process which immediately occurs after the absorbance of light.[1] The transition from vibrational levels in excited state to another vibrational level in lower electronic excited state is called internal conversion (shown by blue curve arrows). This phenomenon takes place due to the overlap of vibrational levels and electronic states energies.[1]

In another transition, excited electrons rapidly decay to the lowest vibrational levels of S_1 and then fluorescence emission occurs from the first singlet excited state to ground electronic state. Generally, the average rate between the time that an electron excites and emits the energy to return to ground state is around 10^{-8} s^{-1}.[1]

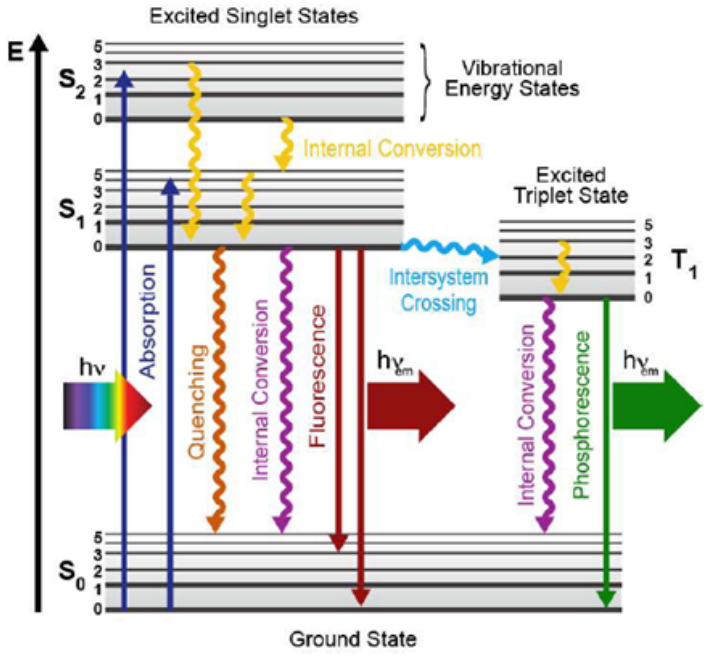

Figure 1.1. Jablonski diagram and energy levels

Besides fluorescence emission, excited electrons in lowest vibrational level in S_1 can undergo intersystem crossing and transfer to first triple state (T_1) and then emission can occur from T_1 to S_0 which is called phosphorescence. This transition from T_1 to S_0 isn't allowed and subsequently phosphorescence emission takes longer than fluorescence emission (millisecond to hours).[1]

1.2. Fluorescence Quantum Yield and Stokes Shift

In addition to lifetime, fluorescence quantum yield is another way to determine the efficiency of fluorescence emission. Quantum yield can be simply calculated by dividing the number of emitted photons to the number of absorbed photons. Fluorescence quantum yield

can be also rewritten as equation 1 where Γ is radiative transition rate and K_{nr} is the sum of nonradiative transition rate.[1]

$$Q = \frac{\Gamma}{\Gamma + k_{nr}}$$

Equation 1.1. Fluorescence quantum yield

As shown in figure 1.2, the wavelength difference between maximum emission band and maximum absorption band defines as Stokes shift. In fact, Stokes shift indicate that the energy of excited fluorophore is lost through molecular vibrations. Temperature, pH, different solvents, and fluorophore are important parameters that can change the value of stokes shift. Basically, larger Stokes shift in a dye increase signal-to-noise ratio and decrease the possibility of self-quenching phenomenon.[2]

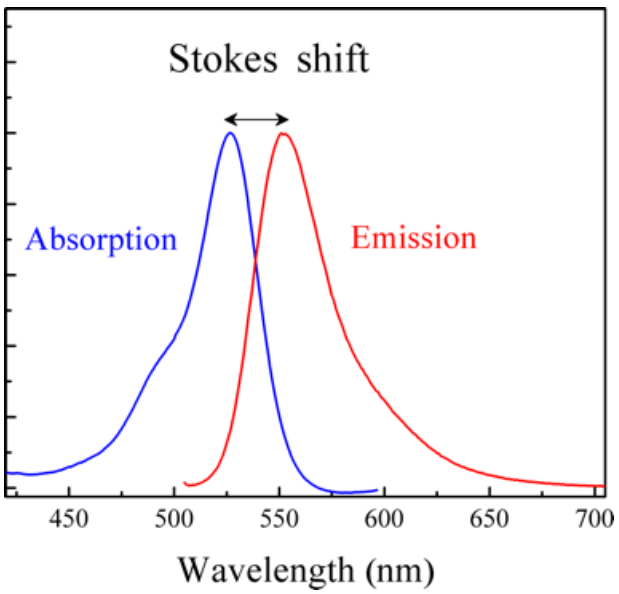

Figure 1.2. Stokes shift in fluorescence

1.3. Fluorescence Signaling Mechanisms

1.3.1 PET

Photo-induced electron transfer (PET) chemical sensors are commonly designed based on three main components, a receptor, a linking spacer, and a fluorophore. As shown in Figure 1.3, PET fluorescence sensors generally work through two OFF and ON modes. In the off mode, the excitation of fluorophore electron from the highest occupied molecular orbital (HOMO) to the lowest unoccupied molecular orbital (LUMO) results in electron transfer from the receptor's HOMO to the fluorophore's HOMO and this phenomenon (photo-induced electron transfer) modulate fluorescence quenching (figure1.3, A). When an analyte binds to the receptor, the energy level of analyte-receptor unit isn't sufficient anymore for electron transfer from receptor's HOMO to vacant HOMO of fluorophore and as a result fluorescence emission occurs (figure 1.3, B).[3]

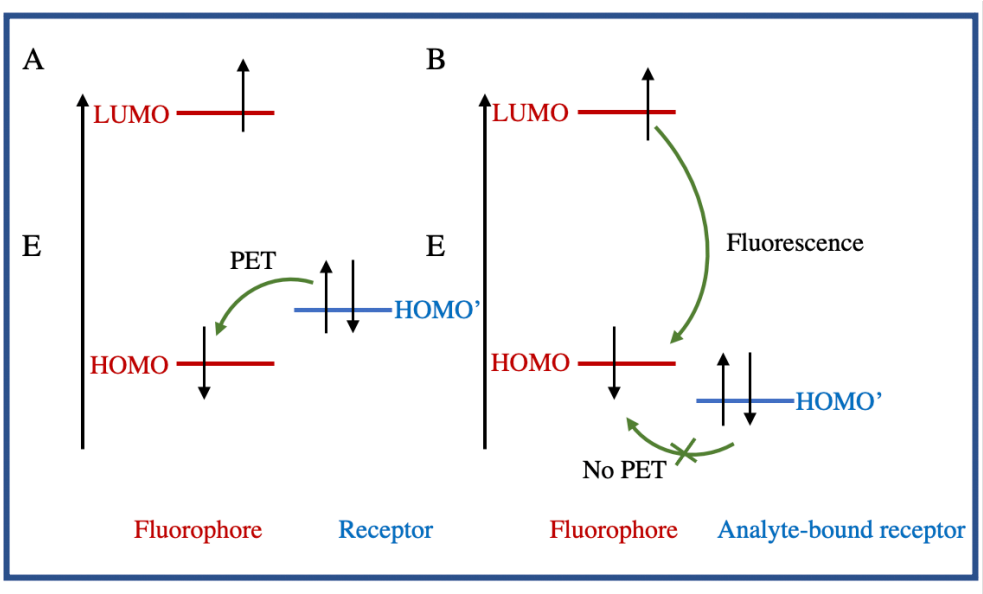

Figure 1.3. Molecular orbital energy diagram illustrating PET mechanism

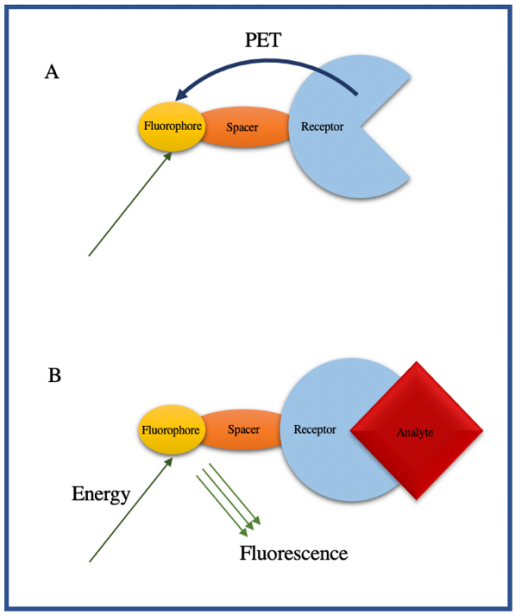

Figure 1.4. A model of PET sensor design (A) analyte-free sensor, (B) analyte-bound model

1.3.2. FRET

The mechanism of fluorescence resonance energy transfer (FRET) is based on the energy transfer from a donor fluorophore in excited state to a ground state accepter through dipole-dipole interaction. This energy transfer occurs when the distance between two donor and acceptor components is approximately less than 10 nanometers. In addition, the emission spectrum of donor and the absorption spectrum of acceptor must show sufficient overlap for an efficient energy transfer, as shown in figure 1.5 (a). Generally, when a FRET sensor binds to an analyte, depending on the distance between donor and acceptor units, electron transfer change, and the sensor undergo either turn-off or turn-on modes. An advantage of FRET fluorescence sensor is the potential of this method to perform ratiometric quantitative analysis.[4]

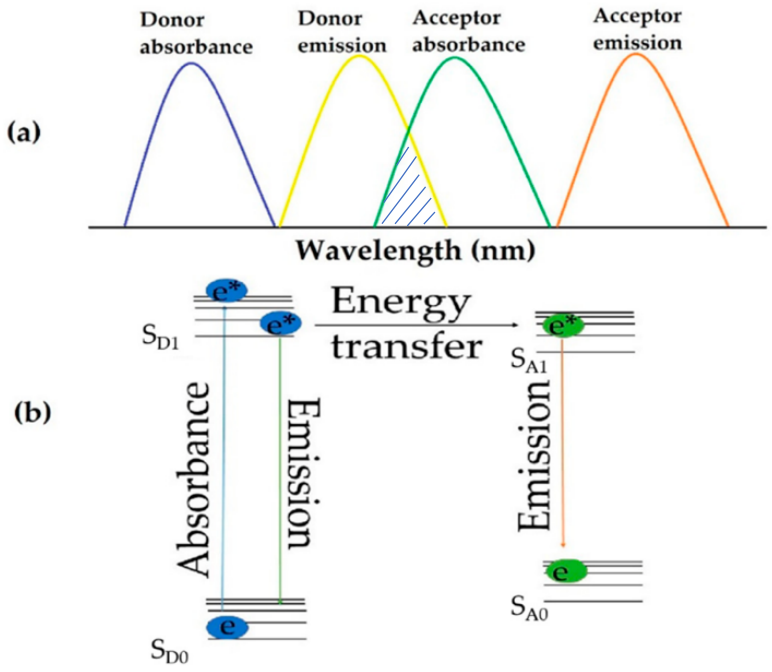

Figure 1.5. Donor absorption and acceptor emission spectra of an ideal donor-acceptor pair (a). Jablonski diagram illustrating the FRET process (b).

1.3.3. Internal Charge Transfer (ICT)

Another important mechanism that is widely used for fluorescence signaling is internal charge transfer (ICT). In the fluorescence sensors based on ICT, a fluorophore is directly bound to a receptor. Upon absorbing light, charge transfer occurs through electron with-drawing and electron-donating groups on this fluorophore-receptor complex and this charge transfer modulates fluorescence emission. Various parameters including pH, fluorophore, solvent, and presence of analyte can disturb charge transfer and change the fluorescence intensity.

For example, Cui and coworkers have reported an ICT ratiometric fluorescence sensor for selective recognition of Cu (II). Strong increase in fluorescence intensity of this sensor

observed upon formation of 1:1 metal-ligand complex. Figure 1.6 shows the structure of synthesized sensor N-butyl-4,5-di[(pyridin-2-ylmethyl) amino]-1,8-naphthalimide.[5]

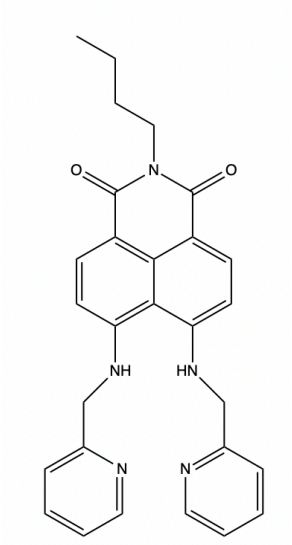

Figure 1.6. N-butyl-4,5-di[(pyridin-2-ylmethyl) amino]-1,8-naphthalimide sensor ICT for Cu (II) sensing.

1.4. Fluorophore

A fluorophore is a small molecule such as proteins, organic compound, or synthetic polymer that absorbs light at a certain wavelength and emits the absorbed light at a longer wavelength. Generally, fluorophores can be categorized into intrinsic and extrinsic classes. Intrinsic fluorophores are naturally fluorescence whereas extrinsic fluorophores need to be modified by reaction with other molecules to show fluorescence properties. Some of the common dye fluorophores are summarized in Table 1.1.[1]

Name	Structure	Color
Fluorescein	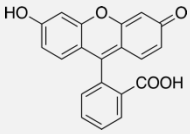	Yellow/ Orange - red
Coumarin	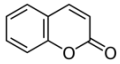	Blue
BODIPY	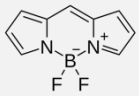	Bright green
Texas red	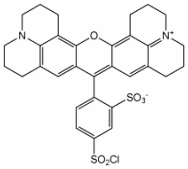	Red
Dansyl Chloride	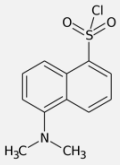	Blue/ Blue - Green
Quinine	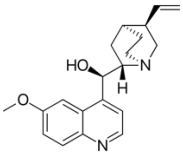	Blue

Table1.1. Most common fluorophores along with their structures and colors.

1.5. Fluorescence Quenching Mechanisms

Fluorescence quenching simply means the decrease in fluorescence intensity and this decrease can be made by numerous molecular interactions including collisional quenching,

molecular rearrangement, and static quenching. Collisional or dynamic quenching occurs when the collision between an excited fluorophore and other molecule in solution (quencher) deactivate the fluorophore. Another quenching mechanism, static quenching, takes place when fluorophore converts to a non-fluorescence complex upon interacting with quenchers.[6]

1.6. Conclusion

Fluorescence is a radiation emitted by specific molecules and the mechanism of fluorescence emission generally describes by Jablonski diagram. There are different mechanisms for designing a fluorescence sensor such as FRET, PET, and ICT. Fluorescence efficiency can be expressed by quantum yield, excited state lifetime, and Stokes shift. Some parameters can affect the efficiency of a fluorescence probe such as pH, fluorophore, and solvent. In next chapter, we will discuss the neurotransmitters' functions and the benefits of developing fluorescence sensors for such molecules.

Chapter 2: Neurotransmitters

2.1. Introduction to Neurotransmitter

Neurotransmitters are endogenous chemical transmitters that allow neuron communication between cells throughout the body. These chemical messengers are associated with various functions in the nervous system, including behavior and cognition. There are many types of neurotransmitters within the body with various roles, including acetylcholine, glutamate, gamma-aminobutyric acid (GABA), glycine, dopamine, norepinephrine, and serotonin. Neurotransmitters can be categorized based on their effects on the target cells into excitatory, inhibitory, and modulatory neurotransmitters.[7] Another way to classify neurotransmitters is according to their chemical structures into five different categories: amino acids, monoamines, neuropeptides, purines, and gasotransmitters.[8] Some important neurotransmitters, their chemical structure and functions are summarized in table 2.1.[9]

Neurotransmitter	Class	Function	Structure
Glutamate	Amino acids	Involved in learning, memory, vision, epilepsy, schizophrenia, excitotoxicity	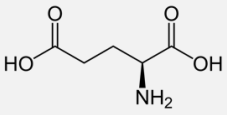
GABA		Effects augmented by alcohol and antianxiety drugs, epilepsy, convulsions	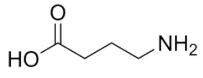
Glycine		Hyperexcitability, uncontrolled convulsions	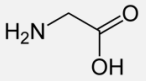

D-serine	Amino acids	Co-agonist of NMDA receptor, schizophrenia	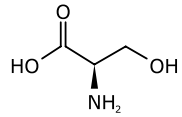
L-Aspartate		Activate NMDA receptor. Co-neurotransmitter with glutamate	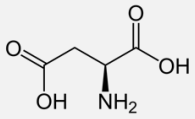
Dopamine	Monoamines	Good feeling, Parkinson's disease and schizophrenia	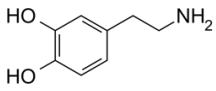
Norepinephrine		Good feeling, depression	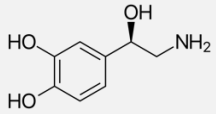
Epinephrine		Fight-or-flight response	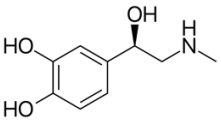
Serotonin		sleep, appetite, nausea, headaches, regulation of mood, schizophrenia, anxiety, and depression	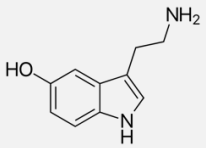
Histamine		Act on G-protein coupled receptors. Involved in Alzheimer's and schizophrenia	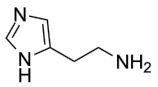

Table 2.1. Neurotransmitters along with their structures and biological functions

Studies show that dysregulations in the concentration of neurotransmitters in synaptic cleft are attributed to a wide range of neurological disorders such as Alzheimer's, schizophrenia, depression, epilepsy, arrhythmias, thyroid hormone deficiency, and Parkinson's disease.[7] For example, the abnormal concentration of dopamine has been directly linked to Parkinson's disease. Thus, the detection of neurotransmitters and monitoring their concentrations in synaptic cleft is necessary to identify the above-mentioned neurological diseases and find

proper therapeutic intervention for them. Over the past few years, numerous techniques have been developed for quantification and qualification analysis of neurotransmitters including nuclear medicine tomography imaging, electrochemical detection (voltammetry and amperometry), separation approaches (high performance liquid chromatography and capillary electrophoresis (CE)), and microanalysis. However, some of these traditional techniques are limited by low sensitivity, cost-effectiveness, and poor spatial resolution. [10]

Conversely, optical sensing methods (chemiluminescence, and fluorescence imaging) provide a high-throughout, non-invasive, and sensitive tool for the detection of small biomolecules such as neurotransmitters in biological fluids. Besides, fluorescence imaging strategies have been widely used to perform both in vitro and in vivo analysis of biomolecules in real time.[8]

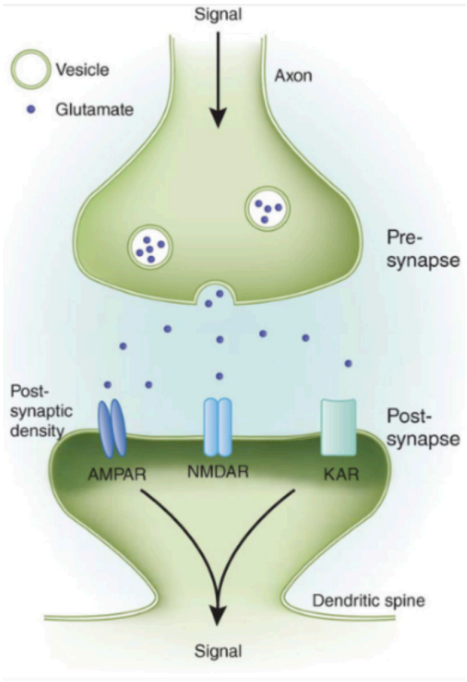

Figure 2.1. Glutamate function in the synaptic cleft

2.1.1. Glutamate

Glutamate as an excitatory neurotransmitter plays an important role in modulating various major functions in the body such as memory, learning, and long-term depression. Therefore, dysregulation of glutamate is directly linked to numerous disorders and diseases. For instance, excessive glutamate in synaptic cleft causes nerve cell death which is called "glutamate-induced excitotoxicity." In other words, excitotoxicity results in neuronal degradation and cascading cell death. These degradations cause neurodegenerative diseases such as Huntington's and Parkinson's diseases.[11] Recently, researchers have found that specific models of schizophrenia could be also related to the abnormal concentration of glutamate.[9]

2.1.2. Gamma-Aminobutyric Acid (GABA)

The primary inhibitory neurotransmitter in central nervous system (CNS) and peripheral nervous system (PNS) is Gamma-Aminobutyric Acid (GABA) which allows hyperpolarization of neurons by controlling ion channels of post synaptic receptors.[12] On the other hand, GABA can also serve as excitatory neurotransmitter in early development of the human body.[13] In other words, GABA prevent hyperpolarization in certain area of the brain such as the neocortex, hippocampus, and hypothalamus. Studies show that various neurological disorders including epilepsy and Parkinson's disease have been related to GABA dysfunction.[9]

2.1.3. Glycine

Glycine is a major inhibitory neurotransmitter that widely presents in various region of CNS including the brainstem and spinal cord. In mammalian CNS, glycine is formed via catalysis reaction of precursor serine via enzyme serine hydroxymethyltransferase (SHMT).[9] Glycine is responsible for modulation of numerous motor control and sensory functions such as spinal cord reflexes.[14]

Glycine and GABA as inhibitory neurotransmitters block the potential action by opening post-synaptic Cl^- channels.[14] Like GABA, glycine has excitatory effects at the early developmental periods and then shifts to inhibitory function at the birth. Disturbance in this shifting process can cause various neurological disorders such as autism.[13] Besides, glycine can act as co-agonist with glutamate at the *N*-methyl-D-aspartate (NMDA) receptors.[15] Recently, researchers found that glycine receptors dysfunction is involved in some diseases including like hypertonia and hyperekplexia.[14]

2.2 Boronic Acid Fluorescence Sensors

2.2.1. Overview

Boronic acid, one of the significant synthetic intermediates in organic chemistry, consists of boron atom, two hydroxyl groups, and one carbon-based substituent. Due to the vacant p-orbital, boron compounds are considered as organic Lewis's acid in a variety of reactions such as the Suzuki coupling reaction, diol protection, and Diels–Alder reaction. In aqueous solution, boronic acid functional group binds covalently to 1,2- or 1,3-diols which results in the formation of five- or six-membered cyclic esters. To understand the design of boronic acid-

based sensors, it is necessary to elaborate the mechanism of interaction between boronic acids and dihydroxy compounds.[16,17,18]

2.2.2. Boronic Acid Binding Constant

In 1959, Lorand and colleagues calculated the equilibrium binding constant between phenyl boronic acid and various dihydroxy compounds using pH-depression technique. In this approach, the pK_a of boron group decrease upon binding to a diol compound.[25] Later, spectroscopic methods revealed a different binding constant in compared with the one had obtained by the pH-depression method.[16] As shown in figure 2.2, boronic acid can react with dihydroxy compounds through two different paths which produce boronic diester and boronate diester respectively. Studies indicate that the calculated binding constant ($K_{eq\text{-}tetrahedral}$) through pH-depression method is corresponded to the second path, the formation of the boronate diester. On the other hand, trigonal boronic acids convert to boronic diester with much lower binding constant ($K_{eq\text{-}trigonal}$). Neither of $K_{eq\text{-}tet}$ and $K_{eq\text{-}tri}$ represent the true binding constant value. Spectroscopic methods calculate the overall binding constant (K_{eq}) (figure 2.3).[16,17]

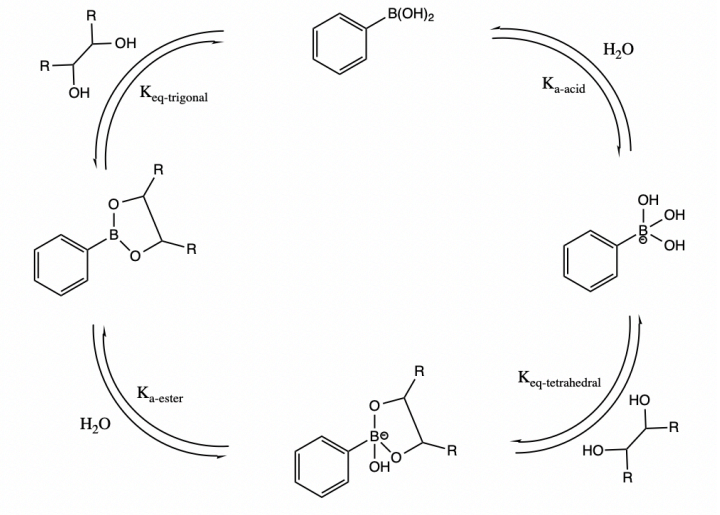

Figure 2.2. Binding mechanism between phenylboronic acid and a diol compound.

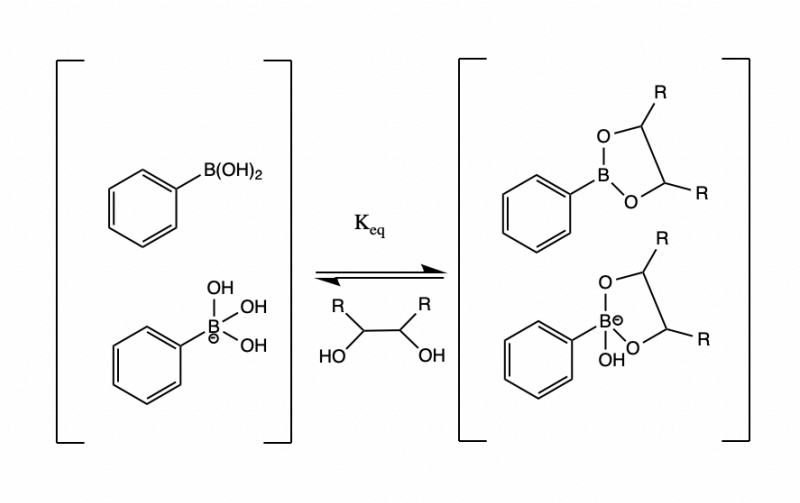

Figure 2.3. Overall binding constant process (K_{eq}).

2.2.3. Boronic Acid Fluorescence Sensors

Boronic acid-based fluorescence sensors are widely used for the detection of saccharides, in particular glucose. In 1992, the first boronic acid-based fluorescence probes for saccharides sensing developed by Czarnik and Yoon. Both anthrylboronic acids sensors (compound 2 and compound 3) have shown great enhancement in fluorescence emission upon binding to glucose and fructose (figure 2.4).[19]

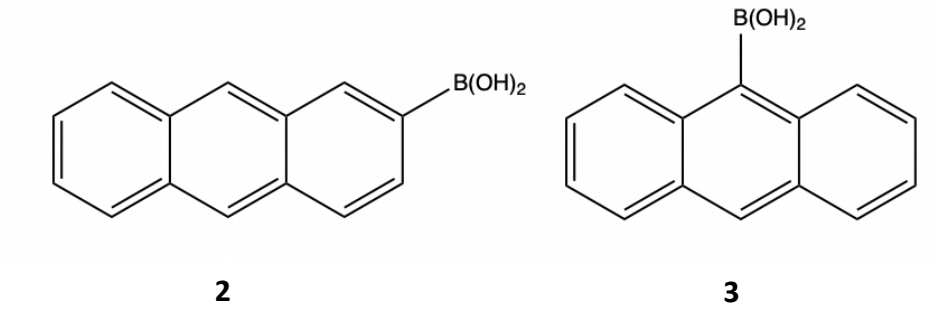

Figure 2.4. Anthrylboronic acids probes for saccharide sensing.

However, these monoboronic acid type of sensors mostly suffer from lack of selectivity and adequate sensitivity. Adding a second boronic acid group for another diol sensing or other type of binding sites strongly increases the affinity of sensors toward the analyte.[16]

Besides sugars, boronic acid fluorescence probes have been utilized for a variety of application such as neurotransmitter sensing, cell imaging, ionic compounds detection, and hydrogen peroxide recognition. Chaicham et al. synthesized a FRET-on/off fluorescence sensor for catecholamine recognition. As shown in figure 2.5, diol group of catecholamine guest linker binds selectively to the probe via boronic acid moiety, and iminium ion formation occurs through aldehyde functional group.[20]

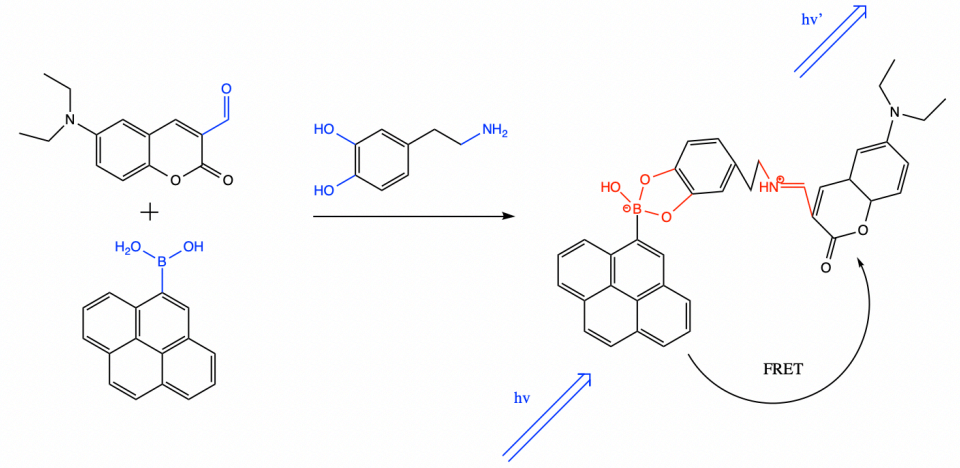

Figure 2.5. A FRET-on based sensor for catecholamine sensing.

2.3. Conclusion

Neurotransmitters are chemical messenger in central nervous system (CNS) and play an important role to regulate various functions in human body that are directly related to our mental and physical health. In this chapter, we have covered neurotransmitter classifications, their

functions and different disorders that are attributed to neurotransmitter dysfunction. Finally, the advantage of using boronic acid fluorescence sensor, their properties, and mechanism of function elaborated in detail.

Chapter 3: Experimental Approach toward Synthesis of Neurosensor 1

3.1. Background

Over the last few years, our group has been working on fluorescence sensors to study amines. Among various fluorophores, sensors with a coumarin-3-aldehyde scaffold interact with amino acids and amines more favorably than other fluorophores. In 2013, Glass et al. worked on a turn-on coumarin aldehyde fluorescence sensor for the detection of norepinephrine in live cells. In this study, neurosensor 521 forms an imine with norepinephrine and shows high increases in fluorescence intensity. The binding constant for catecholamines such as norepinephrine was 10-fold higher than other amines.[21]

To make a more selective sensor, our group developed sensor NS560 which form boronate ester and imine simultaneously when it bonds to amino acids. This new modification enabled the sensor NS560 to sense both alpha and gamma-amino acids with a moderate binding constant while the affinity for other simple amines is negligible.[22]

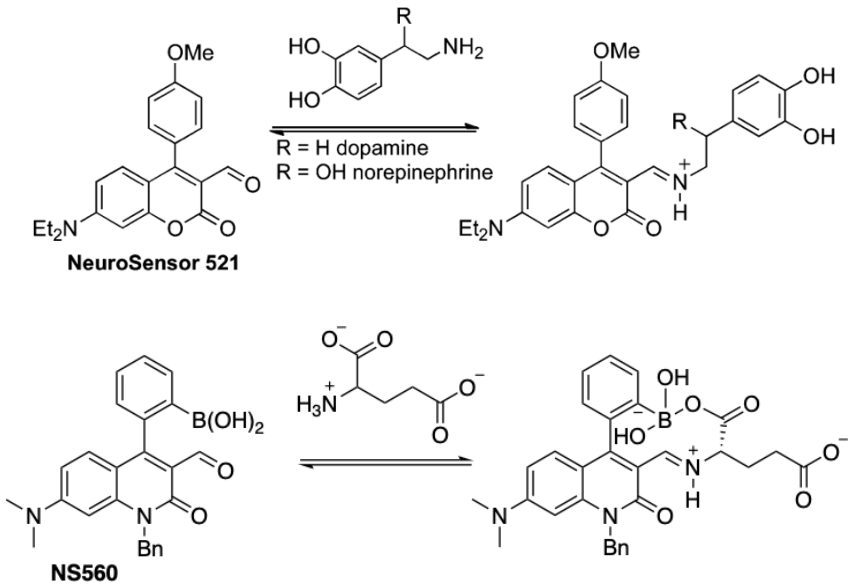

Figure 3.1. Neurosensor 521 and 560 reactions with neurotransmitters.

3.2. Goal

In this project, we plan to develop a sensor based on NS560 for sensing only gamma-amino acid, glutamate, in human cells. According to our modeling results, changing the position of boronic acid and modifying the aryl group helps us to build a sensor with a higher affinity to glutamate. Calculations indicate that the angle between the aryl group and fluorophore highly affects the binding affinity. Replacing the aryl group with naphthyl fixes this angle at 89°, and in this configuration only gamma-amino acids such as glutamate and GABA can fit in binding site. Figure 3.2 shows our proposed neuro-sensor 1 for selective recognition of gamma-amino acids neurotransmitter, glutamate and GABA.

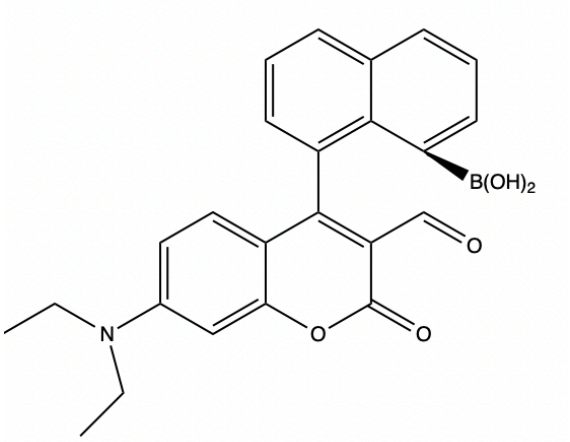

Figure 3.2. Designed fluorescence neurosensor1 for the detection of gamma amino acids.

3.3. Synthesis of Neurosensor 1

3.3.1 First Synthesis Approach

7-diethylamino 4-hydroxycoumarin

Bis(2,4,6-trichlorophenyl) malonate was synthesized through reacting 2,4,6-trichlorophenol with malonic acid in the presence of phosphorous (V) oxychloride ($POCl_3$). White compound was formed and stored for the next step.

7-diethylamino 4-hydroxycoumarin was prepared by reacting bis(2,4,6-trichlorophenyl) malonate with diethylamino phenol and in toluene. The mixture was heated at 95°C for 3 hrs. The green product was obtained with 70% reaction yield.

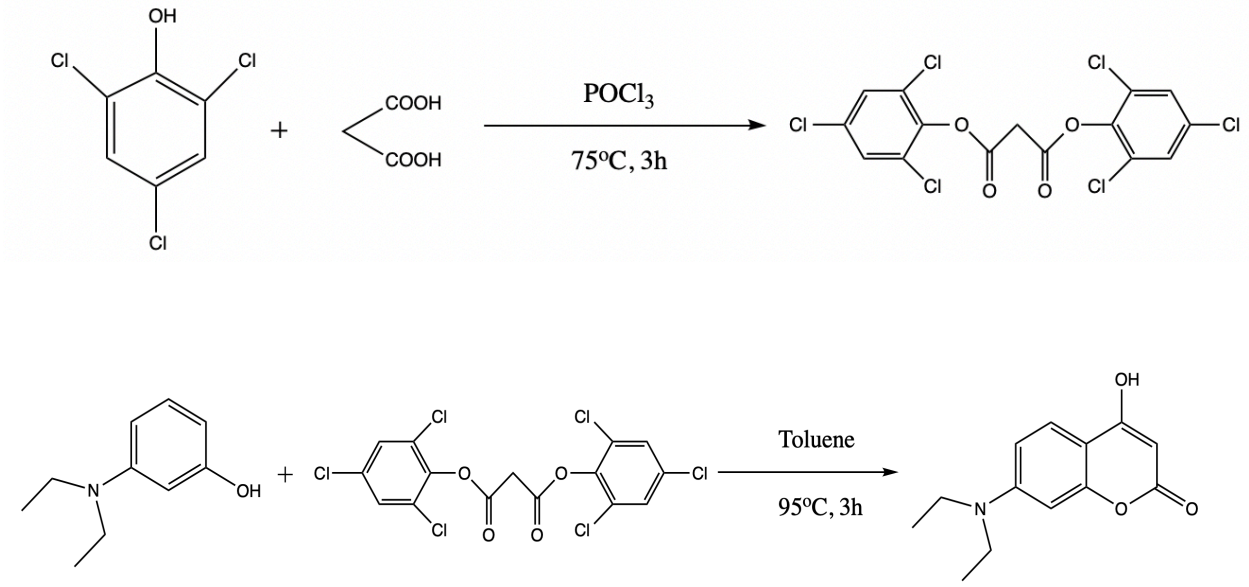

Scheme 3.1. Synthesis route of 7-diethylamino 4-hydroxycoumarin

Naphthalene diboronic acid:

Naphthalene diboronic acid was prepared by the four-steps synthesis route. Diiodonaphthalene was synthesized through Sandmeyer reaction. between 1,8diaminonaphthalene reacts with sodium nitrite to produce the intermediate diazonium ion under acidic condition. Then, diazonium ion can undergo substitution reaction with potassium iodide. The white diiodonaphthalene was obtained with 68% reaction yield.

Diiodonaphthalene was used in following reaction with butyl lithium as organometallic reagent and trimethyl borate. This reaction is temperature sensitive and must be kept at -78°C for the entire time. Naphthalene diboronic acid was successfully synthesized with 45% yield.

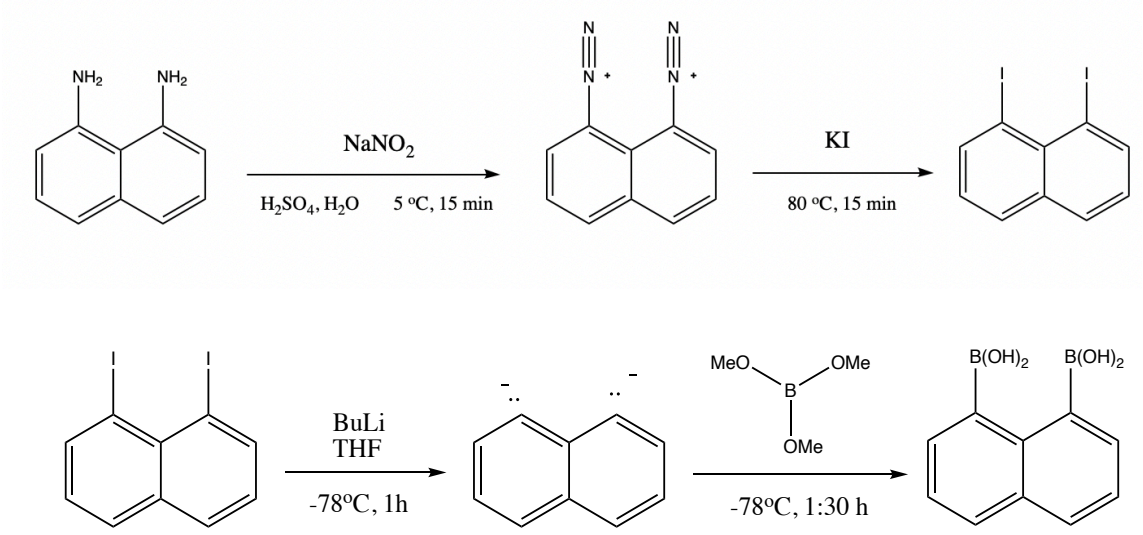

Scheme 3.2. Synthesis route of naphthalene diboronic acid

7-diethylamino 4-arylcoumarin [3]

This step is based on the Suzuki-Miyaura[23] reaction which is a palladium-catalyzed cross coupling between organoboronic acid compound and halides. Commercial phenyl boronic acid

undergoes cross- coupling reaction with 7-diethylamino 4-hydroxycoumarin to produce 7-diethylamino 4-arylcoumarin. This is a test reaction to optimize all condition such as temperature, base, catalyst, and reaction time. Then we move forward and replace phenyl boronic acid with synthesized naphthalene diboronic acid.

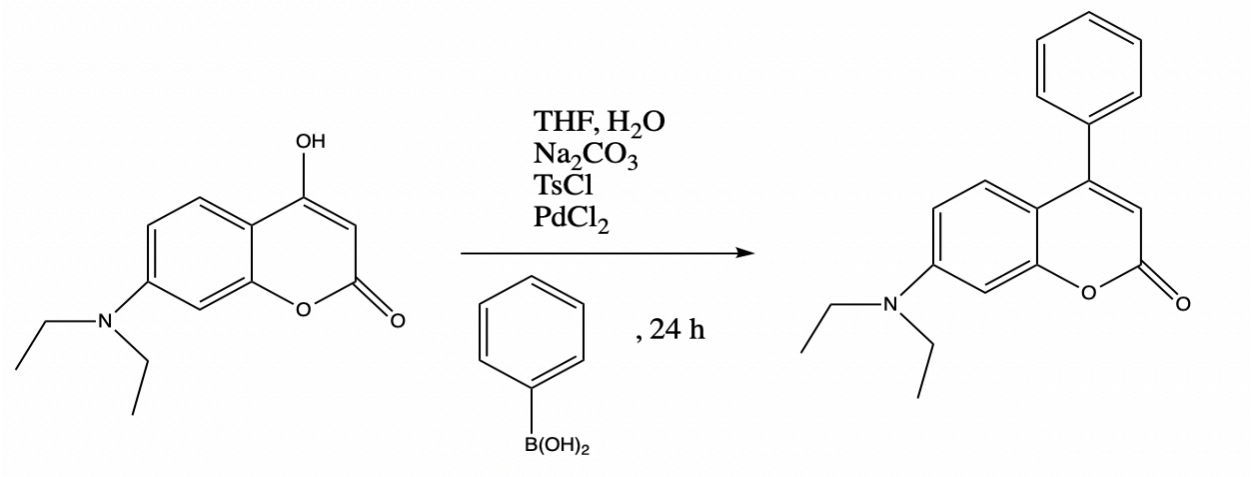

Scheme 3.3. Synthesis route of 7-diethylamino 4-arylcoumarin

Compound 1

After 7-diethylamino 4-arylcoumarin has successfully synthesized, a cross-coupling reaction was done again using naphthalene diboronic acid instead of aryl boronic acid.

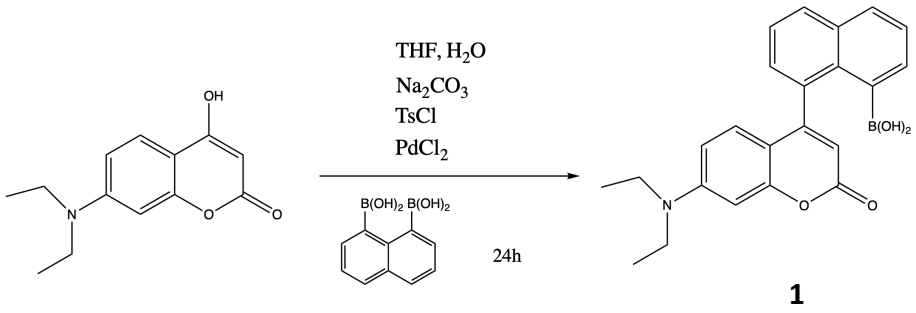

Scheme 3.4. Synthesis route of designed fluorescence sensor

NMR data and fluorescence titrations results indicate that boronic acid functional group is lost during synthesis of compound 1. The structure of synthesized product is shown in figure 3.3.

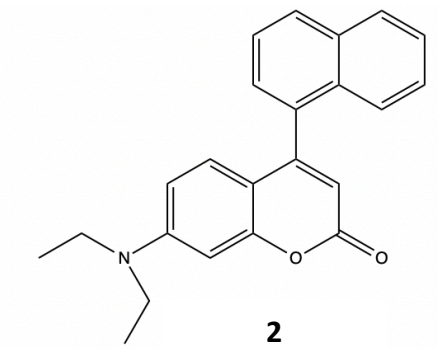

Figure 3.3. The structure of cross-coupling reaction product

To confirm missing boronic acid group, we decided to formylate compound 2 and perform some titration experiments. Formylation reaction was done on compound 2 through Vilsmeier-Haack reaction, as shown in scheme 3.5.

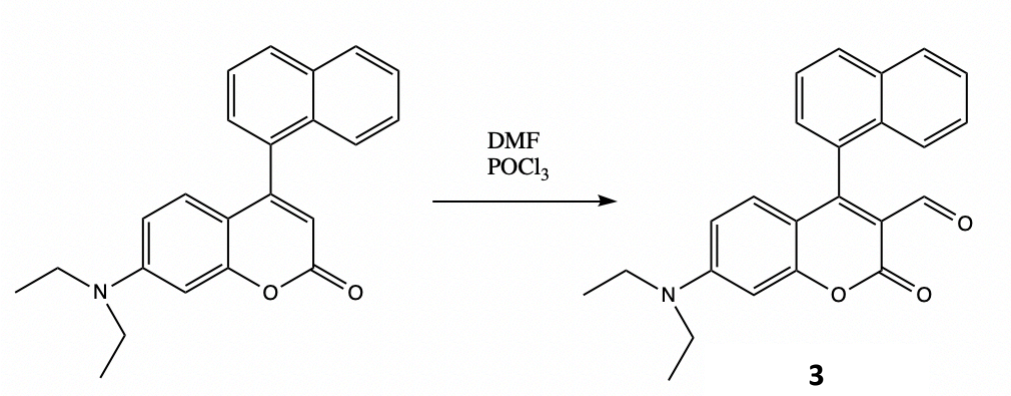

Scheme 3.5. Vilsmeier-Haack reaction

Binding constants (K_D) values indicate that how tightly a target molecule binds to a fluorescence sensor. Binding constant calculated from fluorescence and UV-Vis titrations of compound 3 with glutamate, GABA, and glycine amino acids indicate relatively low values which are corresponded to only iminium ion formation. (Figures 3.4, 3.5, 3.6, 3.7, 3.8, and 3.9)

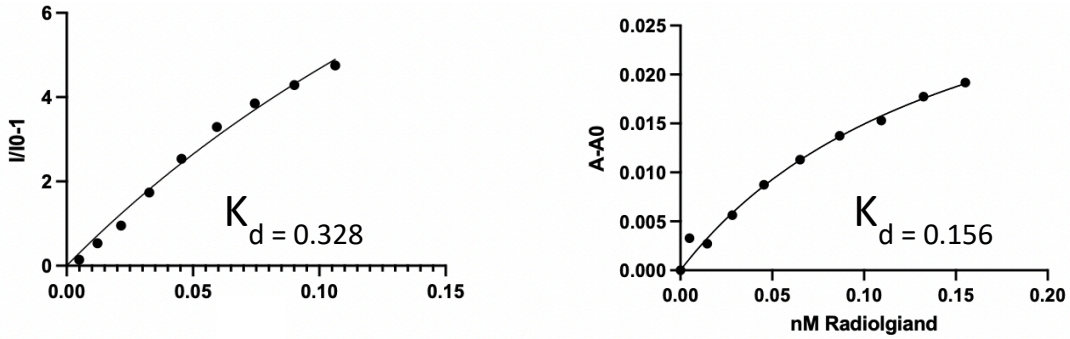

Figure 3.4. Binding constants calculated through fluorescence (A) and UV-Vis (B) titrations of compound 3 with glutamate in buffer (10mM HEPES, 120mM NaCl, pH= 5, [Compound 3] = 20μM, [glutamate] = 0.5mM).

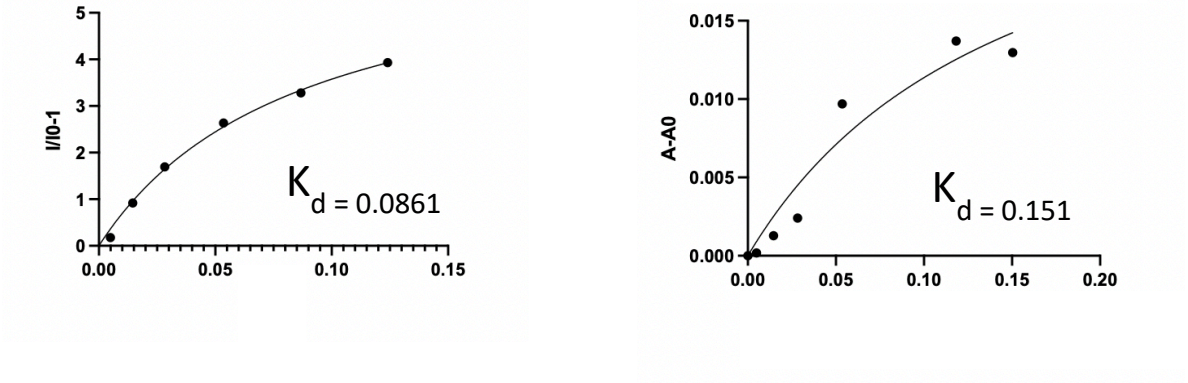

Figure 3.5. Binding constants calculated through fluorescence (A) and UV-Vis (B) titrations of compound 3 with glycine in buffer (10mM HEPES, 120mM NaCl, pH= 5, [Compound 3] = 20μM, [Glycine] = 0.5mM).

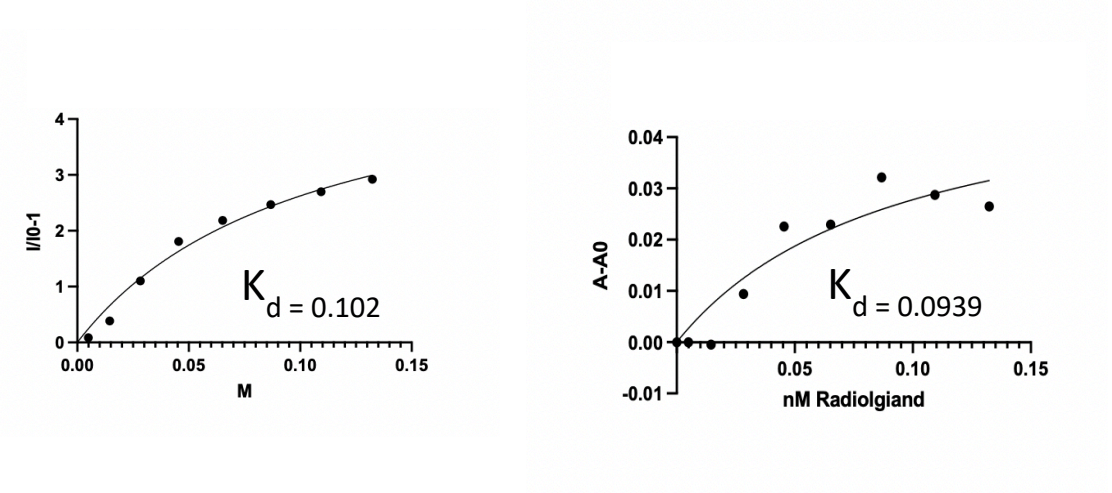

Figure 3.6. Binding constants calculated through fluorescence (A) and UV-Vis (B) titrations of compound 3 with Glycine in buffer (10mM HEPES, 120mM NaCl, pH= 7.4, [Compound 3] = 20μM, [Glycine] = 0.5mM).

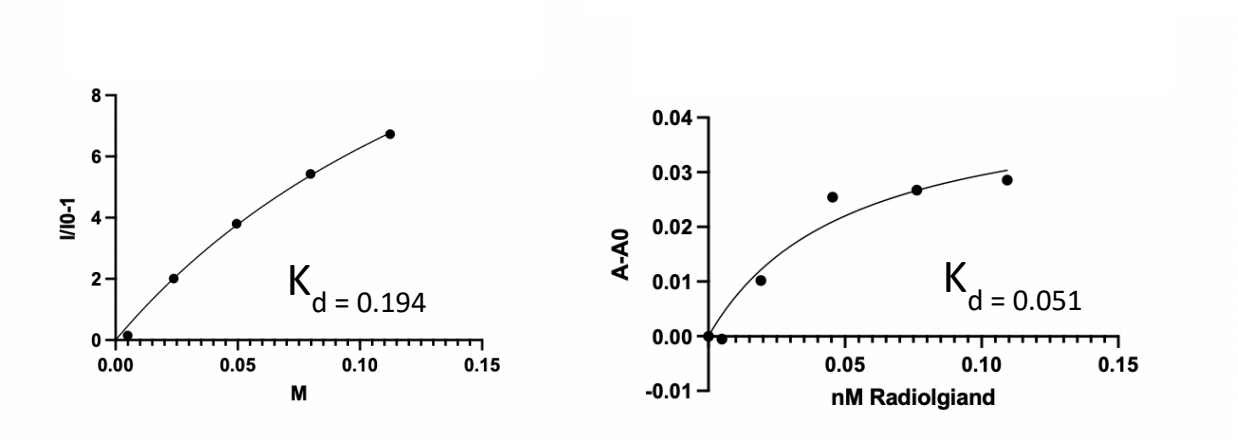

Figure 3.7. Binding constants calculated through fluorescence (A) and UV-Vis (B) titrations of compound 3 with GABA in buffer (10mM HEPES, 120mM NaCl, pH= 5, [Compound 3] = 20μM, [GABA] = 0.5mM).

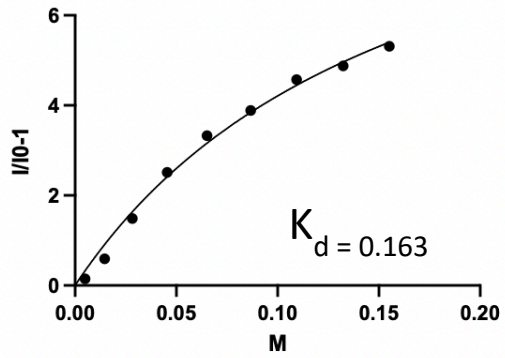

Figure 3.8. Binding constants calculated through fluorescence titration of compound 3 with glutamate in buffer (10mM HEPES, 120mM NaCl, pH= 7.4, [Compound 3] = 20μM, [glutamate] = 0.5mM).

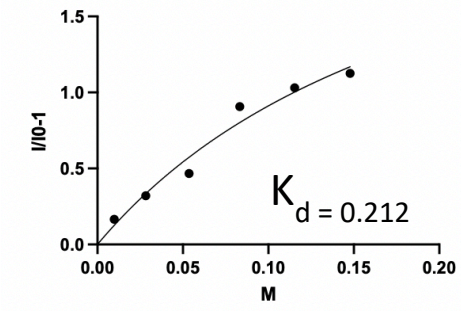

Figure 3.9. Binding constants calculated through fluorescence titration of compound 3 with GABA in buffer (10mM HEPES, 120mM NaCl, pH= 7.4, [Compound 3] = 20μM, [GABA] = 0.5mM).

3.3.2. Alternative Synthesis Approach

The actual chemical structure of naphthalene diboronic acid is shown in figure 3.10. In this configuration, we lose both boronic acid groups during coupling reaction under any conditions. To overcome this challenge, we have proposed following alternative approach to synthesis Neurosensor1.

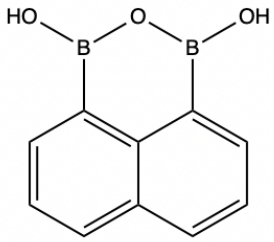

Figure 3.10. Chemical structure of Naphthalene boronic acid.

7-diethylamino 4-bromocoumarin

In first step in this approach, 7-diethylamino 4-hydroxycoumarin was reacted with tetrabutylammonium bromide and phosphorous pentoxide to produce 7-diethylamino 4-bromocoumarin. The product (7-diethylamino 4-bromocoumarin) was obtained with 65% yield.

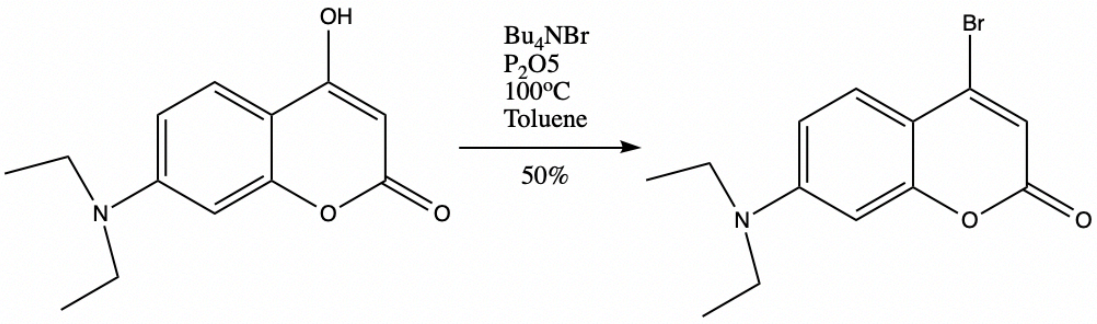

Scheme 3.6. Synthesis route of 7-diethylamino 4-bromocoumarin

7-diethylamino 4-diboronic ester coumarin

7-diethylamino 4-diboronic ester coumarin was prepared through Miyaura borylation[24] reaction in which cross-coupling occurs between bis(pinacolato)diboron (B_2pin_2) and aryl halides. Finally, the 7-diethylamino 4-diboronic ester successfully has synthesized by an overall yield of 40%.

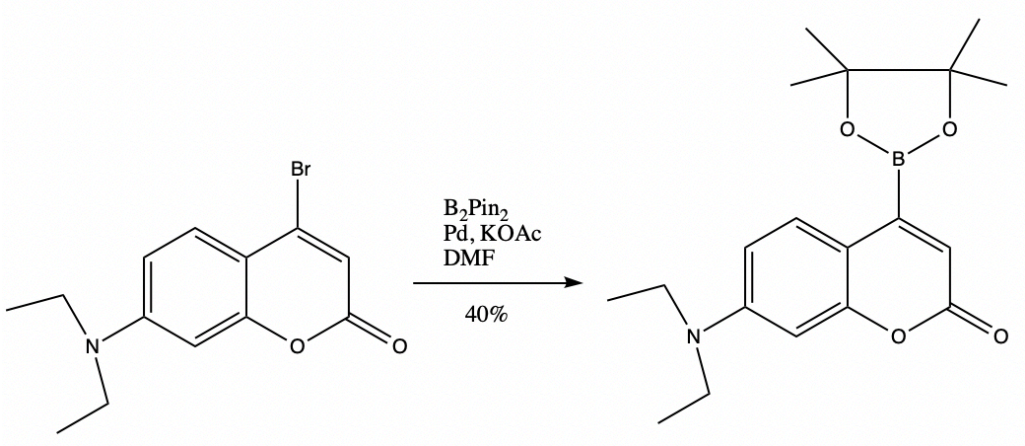

Scheme 3.7. Synthesis of 7-diethylamino 4-diboronic ester coumarin

Compound 4

We are currently optimizing cross-coupling reaction between 7-diethylamino 4-diboronic ester and diiodonaphthalene (scheme 3.8).

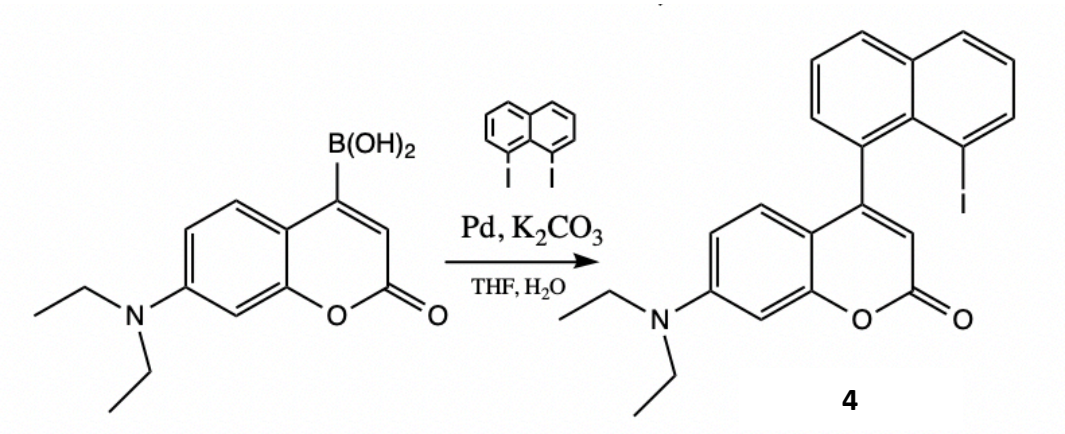

Scheme 3.8. Synthesis of compound 4

3.3.3. Future Work

Next step through the synthesis of neurosensor 1 will be done by done reacting compound 4 with Butyl lithium in presence of tri methyl borate (scheme 3.9). Then compound 5 undergo formylation by Vilsmeier-Haack reaction (scheme 3.10) and final product will be used for fluorescence titration with three glutamate, GABA, and glycine amino acids.

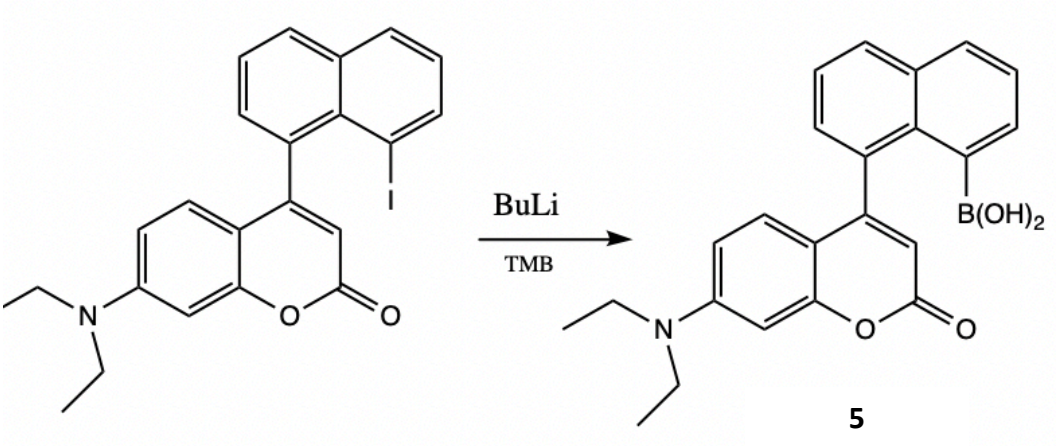

Scheme 3.9. Synthesis of compound 5

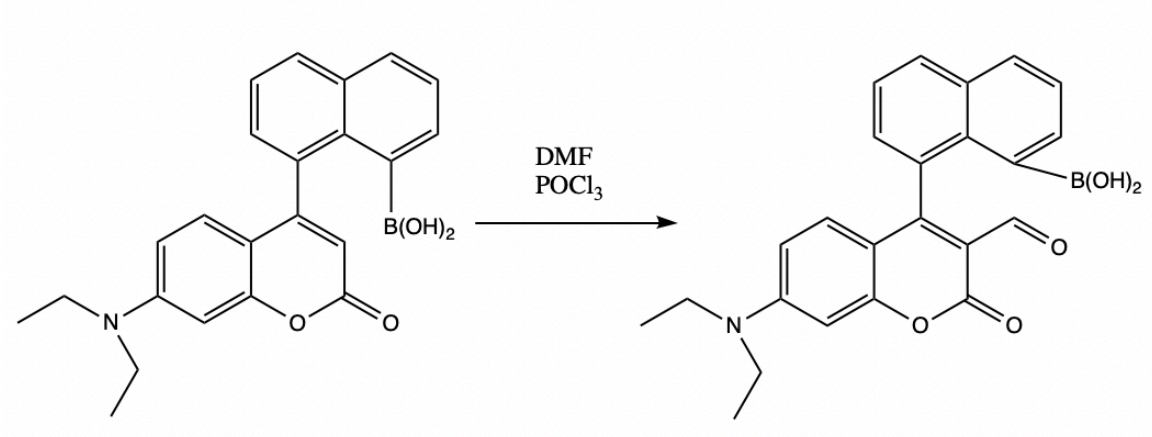

Scheme 3.10. Synthesis of neurosensor 1

Supplemental Information

Synthesis of 7-diethylamino 4-hydroxycoumarin:

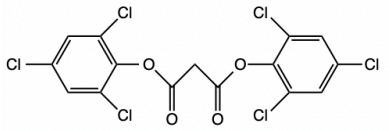

A mixture of 15.8 g of 2,4,6-trichlorophenol, 4.16 g of malonic acid, and 20 mL of phosphorous(v) oxychloride was placed in a round bottom flask. Then, the flask was heated at 75°C for 3 hrs. After 3h, 10 mL of saturated sodium bicarbonate solution was added to the mixture at room temperature. The white product was dried and kept at room temperature for next step.

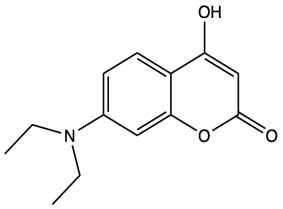

9.6 g of bis(2,4,6-trichlorophenyl) malonate was transferred to another flask. Then 3.3 g of diethylamino phenol and 50 mL of toluene were added to the flask. The mixture was heated at 95°C for 3 hrs. The product was washed with toluene up to 5 times and dried by rotary evaporator.

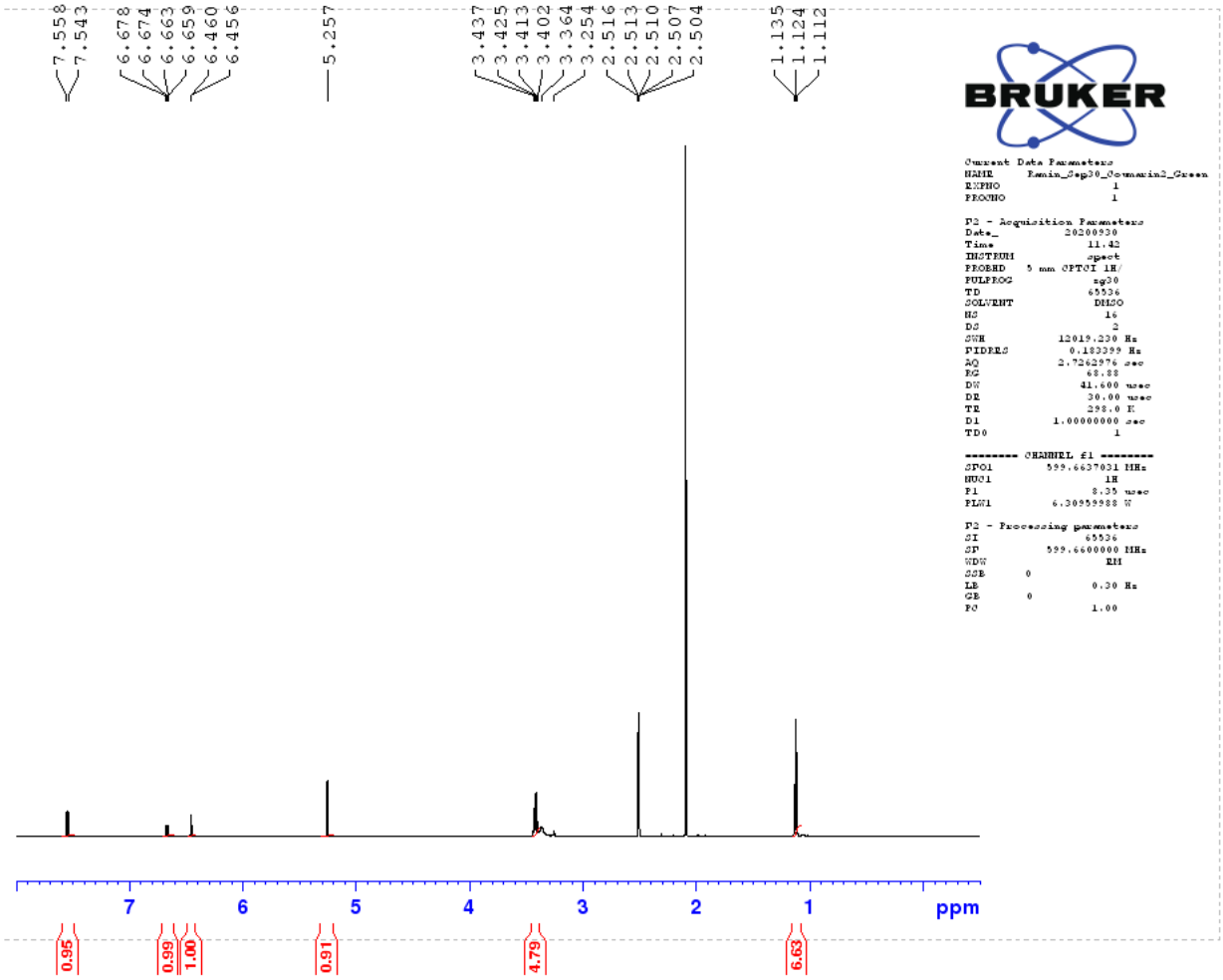

^{1}HNMR (600MHz, $CDCl_3$), δ 7.543-7.558 (d, 1H, J = 9.0 Hz), 6.659-6.678 (m, 1H), 6.456-6.460 (d, 1H, J = 2.4 Hz), 5.257 (s, 1H), 3.364-3.437 (m, 4H), 1.112-1.135 (t, 6H, J = 6.6 Hz).

Synthesis of diiodoaphthalene:

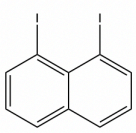

7 g of 1,8diaminonaphthalene was dissolved in a mixture of 15 mL of sulfuric acid and 50 mL of cold DI water. The mixture was kept at 5° C. Then, the solution of 9 g sodium nitrite in 50 mL of water was added slowly to the reaction flask. After 5 minutes, potassium iodide solution (45 g of potassium iodide in 60 mL of water) was added to the reaction. The mixture was heated at 80° C for 10 minutes and rapidly was cooled down to 20° C. 1,8 diiodonaphthalene was filtered and washed by diethyl ether. Chromatography purification was done by 80% DCM/diethyl ether.

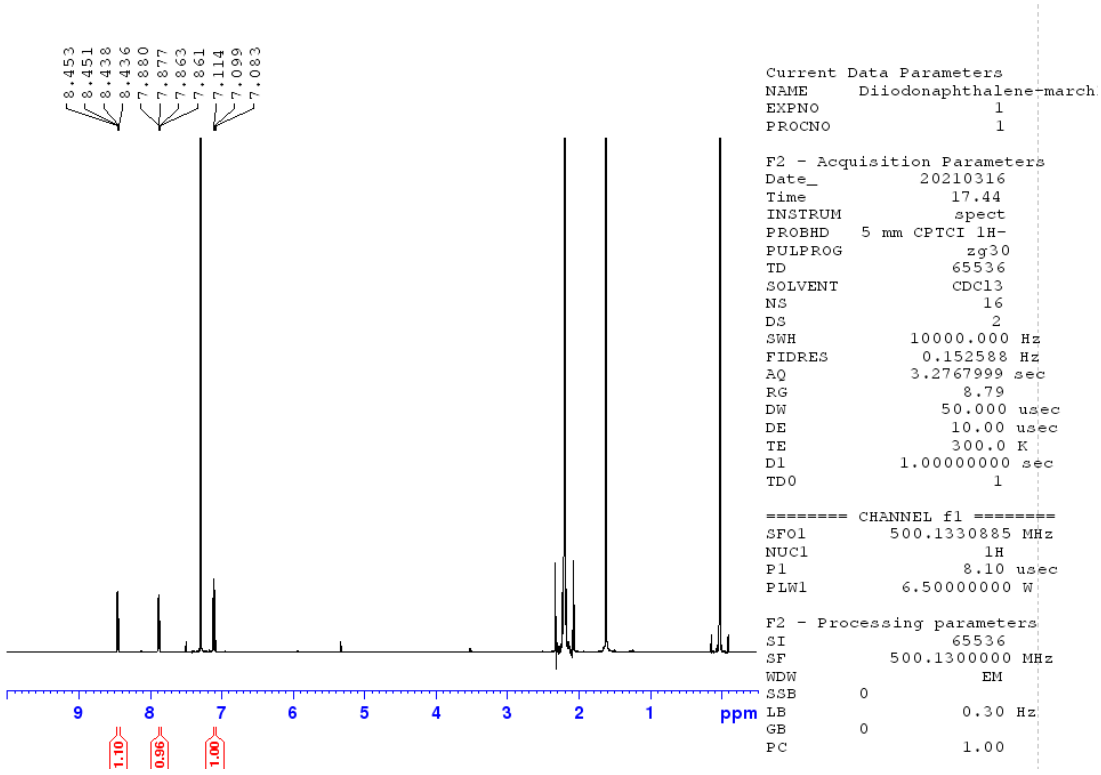

^{1}HNMR (500MHz, $CDCl_3$), δ 8.436-8.453 (d, 2H, J = 8.5 Hz), 7.861-7.880 (d, 2H, J = 9.5 Hz), 7.083-7.114 (dd, 2H, J = 10.5, 15.5 Hz).

Synthesis of naphthalene diboronic acid:

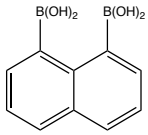

Step2: 75 mg of diiodonaphthalene was dissolved in 3 mL of THF and degassed for 10 minutes at -78°C. Then, 0.45 mL of n-BuLi was added to the mixture and the reaction was kept at -78° C. After hour, 0.25 mL of trimethyl borate was added to reaction mixture. After 2 hrs, the flask was transferred to room temperature, and 2 mL of saturated ammonium chloride was added. Then, the compound was recrystallized using 70% dichloromethane:hexane. Finally, the product was dried and stored for future purposes.

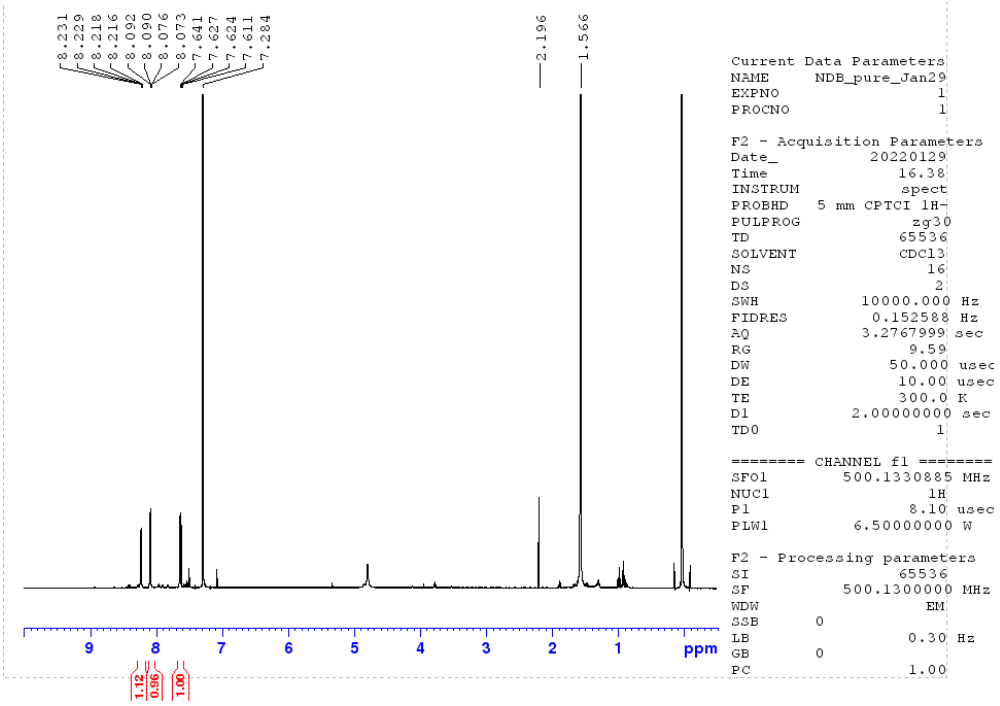

^{1}HNMR (500MHz, $CDCl_3$), δ 8.216-8.231 (d, 2H, J = 7.5 Hz), 8.076-8.092 (dd, 2H, J = 8.2, 9.5 Hz), 7.611-7.641 (d, 2H, J = 15 Hz).

Synthesis of 7-diethylamino 4-arylcoumarin:

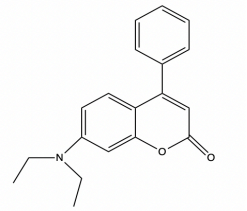

A solution of 30 mg 7-diethyl amino 4-hydroxy coumarin and 27.5 mg of TsCl was prepared in 2.1 mL of 1:20 THF: H_2O and degassed for 1 h. Then, 19 mg of phenylboronic acid, 41.3 mg of sodium carbonate, and 1.15 mg of palladium catalyst were added to the mixture and stirred for 24 h at 120°C. When the product was formed, saturated sodium chloride was added to the mixture. The product was dried, and column chromatography was done in two steps. 1) 80% DCM/diethyl ether. 2) 97:03, 95:05, 90:10, methylene chloride: ethyl acetate.

Synthesis of compound 1:

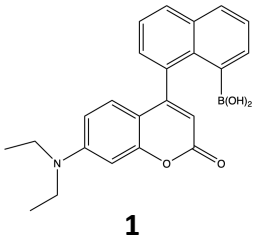

1

A solution of 1eq 7-diethyl amino 4-hydroxy coumarin and 1.1 eq of TsCl was prepared in 3 mL of 1:20 THF: H2O and degassed for 1 h. Then, 1.1 eq of naphthalene diboronic acid, 4 eq of sodium carbonate, 0.15 eq sphos, and 0.05 eq of palladium catalyst were added to the mixture and stirred for 24 h at 120°C. When the product was formed, saturated sodium chloride was added to the solution. The product was dried and purified in two steps. 1) 80% DCM/diethyl ether. 2) 97:03, 95:05, 90:10, methylene chloride: ethyl acetate. To obtain

compound 3, compound 2 formylated through vilsmeier-haack reaction in presence of DMF and $POCl_3$.

Synthesis of compound 3:

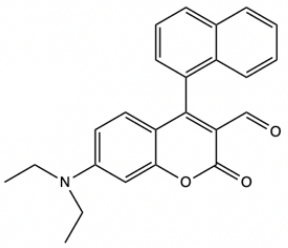

3

Reagent solution: 7 mL of DMF was placed in a flame-dried flask and 3.8 mL of phosphorous (V) oxychloride was slowly added to the flask at 0°C. The mixture was stirred at room temperature for 45 minutes.

10 mg of compound 3 was dissolved in 1 mL DMF and stirred at room temperature for 15 minutes (under nitrogen gas). 0.5 mL of reagent solution was added, and the entire mixture was stirred for 12 hrs. Then, 10 mL of ice DI water was added to the reaction flask and the mixture was basified with saturated sodium hydrogen carbonate until pH= 4. Extraction was done with 2×10 mL DCM. The product was obtained by 36% reaction yield.

Synthesis of 7-diethylamino 4-bromocoumarin:

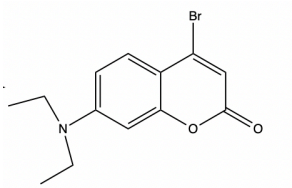

210.00 mg of 7-diethylamino 4-hydroxycoumarin was dissolved in 4 mL toluene and stirred at 100°C for 10 minutes (under nitrogen gas). 580.43 mg of tetrabutylammonium bromide was added to above mixture and stirred for another 10 minutes at 100°C. 766.73 mg of phosphorous pentoxide was added, and the entire mixture refluxed for 3h at 100°C. The organic layer was separated, and the lower layer was extracted by a mixture of 50% toluene and 50% water. The combined organic layer was washed with 10 mL DI water, 2×10 mL 5% sodium hydrogen carbonate, and 20 mL brine solution respectively. The final solution was dried over saturated magnesium chloride and concentrated by rotary evaporator. The product (7-diethylamino 4-bromocoumarin) was obtained with 65% yield.

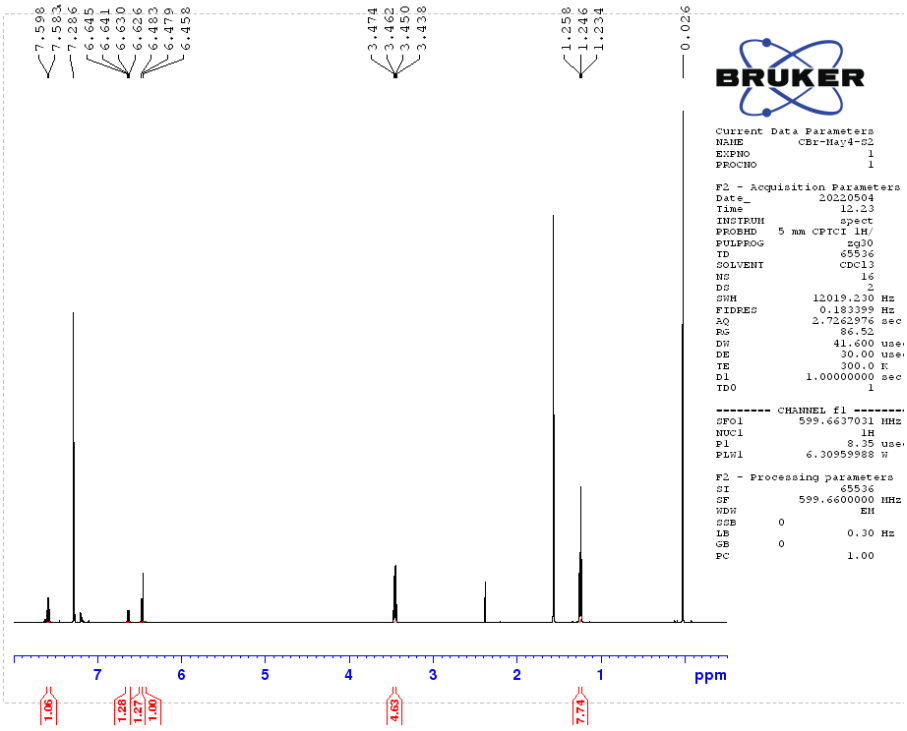

^{1}HNMR (600MHz, $CDCl_3$), δ 7.583-7.598 (d, 1H, *J* = 9.0 Hz), 6.626-6.645 (m, 1H), 6.479-6.483 (d, 1H, *J* = 2.4 Hz), 6.458 (s, 1H), 3.438-3.474 (m, 4H), 1.234-1.258 (t, 6H, *J* = 7.2 Hz).

Synthesis of 7-diethylamino 4-diboronic ester coumarin:

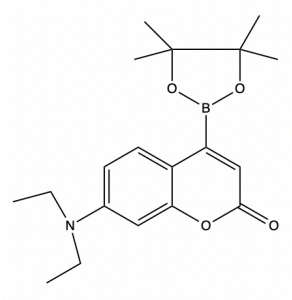

130 mg of 7-diethylamino 4-bromocoumarin, 134 mg of bis(pinacolato)diboron, 151.15 mg of potassium acetate, and 32.19 mg of [1,1'-Bis(diphenylphosphino)ferrocene] palladium (II) dichloride were added to a flame dried round bottom flask and dissolved in 5 mL of DMF. Mixture was stirred for 1h at room temperature and another 24h at 90°C. then 20 mL of ethyl acetate was added to the solution and the entire mixture was filtered through Celite. Finally, the solution was concentrated by rotary evaporator and 7-diethylamino 4-diboronic ester successfully synthesized by an overall yield of 40%.

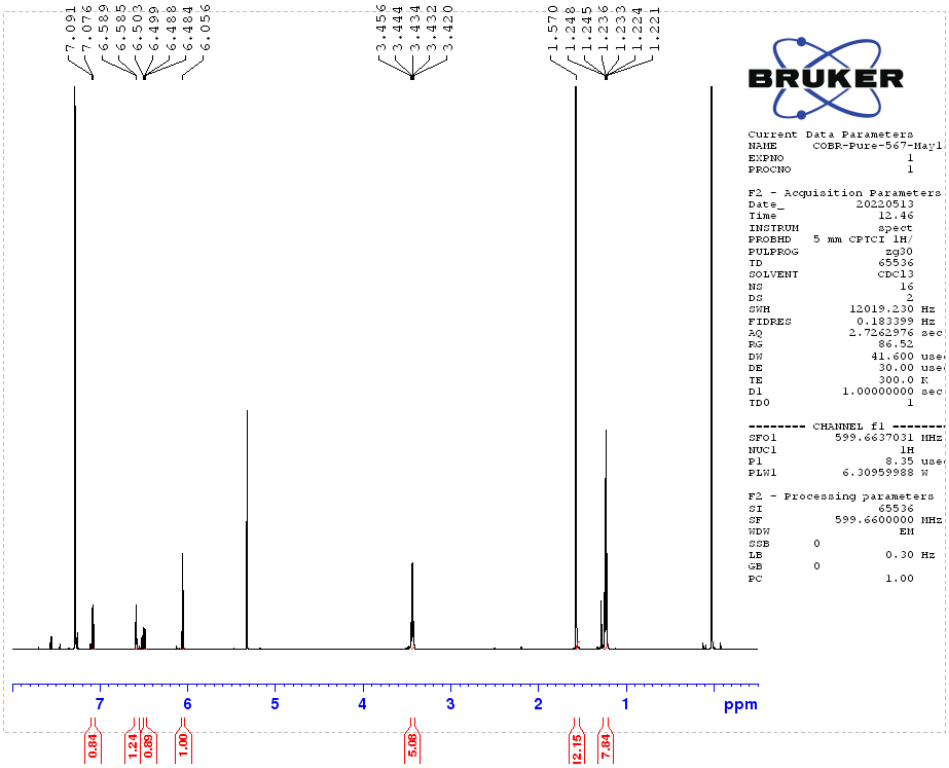

^{1}HNMR (600MHz, $CDCl_3$), δ 7.076-7.091 (d, 1H, *J* = 9.0 Hz), 6.585-6.589 (d, 1H, *J* = 2.4 Hz), 6.484-6.503 (m, 1H), 6.056 (s, 1H), 3.438-3.474 (m, 4H), 1.233-1.245 (t, 6H, *J* = 3.6 Hz), 1.570 (s, 12H).

References

(1) Joseph R. Lakowicz. (2006). Principles of Fluorescence Spectroscopy.

(2) Ren, T. B., Xu, W., Zhang, W., Zhang, X. X., Wang, Z. Y., Xiang, Z., Yuan, L., & Zhang, X. B. (2018). A General Method to Increase Stokes Shift by Introducing Alternating Vibronic Structures. Journal of the American Chemical Society, 140(24), 7716–7722.

(3) Pradhan, T., Jung, H. S., Jang, J. H., Kim, T. W., Kang, C., & Kim, J. S. (2014). Chemical sensing of neurotransmitters. Chemical Society Reviews, 43(13), 4684–4713.

(4) Jalihal, A., Le, T., Macchi, S., Krehbiel, H., Bashiru, M., Forson, M., & Siraj, N. (2021). Understanding of Förster Resonance Energy Transfer (FRET) in Ionic Materials. Sustainable Chemistry, 2(4), 564–575.

(5) Li, Y., Lin, H., & Lin, H. (2010). Ratiometric and selective fluorescent sensor for F - based on intramolecular charge transfer (ICT). Journal of Fluorescence, 20(6), 1299–1305.

(6) J.R. Albani. (2004). Structure and Dynamics of Macromolecules: Absorption and Fluorescence Studies. Chapter 4, 141-192.

(7) Arumugasamy, S. K., Chellasamy, G., Gopi, S., Govindaraju, S., & Yun, K. (2020). Current advances in the detection of neurotransmitters by nanomaterials: An update. TrAC - Trends in Analytical Chemistry, 123, 115766.

(8) Sustainable Pradhan, T., Jung, H. S., Jang, J. H., Kim, T. W., Kang, C., & Kim, J. S. (2014). Chemical sensing of neurotransmitters. Chemical Society Reviews, 43(13), 4684–4713.

(9) Niyonambaza, S. D., Kumar, P., Xing, P., Mathault, J., Koninck, P. De, Boisselier, E., Boukadoum, M., & Miled, A. (2019). A Review of neurotransmitters sensing methods for neuro-engineering research. Applied Sciences (Switzerland), 9(21), 1–31.

(10) Ghasemi, F., Hormozi-Nezhad, M. R., & Mahmoudi, M. (2016). Identification of catecholamine neurotransmitters using fluorescence sensor array. Analytica Chimica Acta, 917, 85–92.

(11) Dong, X. X., Wang, Y., & Qin, Z. H. (2009). Molecular mechanisms of excitotoxicity and their relevance to pathogenesis of neurodegenerative diseases. Acta Pharmacologica Sinica, 30(4), 379–387.

(12) Miller, M. W. (2019). Gaba as a neurotransmitter in gastropod molluscs. Biological Bulletin, 236(2), 144–156.

(13) Ito, S. (2016). GABA and glycine in the developing brain. Journal of Physiological Sciences, 66(5), 375–379.

(14) Gundersen, R. Y., Vaagenes, P., Breivik, T., Fonnum, F., & Opstad, P. K. (2005). Glycine - An important neurotransmitter and cytoprotective agent. Acta Anaesthesiologica Scandinavica, 49(8), 1108–1116.

(15) Cummings, K. A., & Popescu, G. K. (2015). Glycine-dependent activation of NMDA receptors. Journal of General Physiology, 145(6), 513–527.

(16) Fang, H., Kaur, G., & Wang, B. (2004). Progress in boronic acid-based fluorescent glucose sensors. Journal of Fluorescence, 14(5), 481–489.

(17) Fang, G., Wang, H., Bian, Z., Sun, J., Liu, A., Fang, H., Liu, B., Yao, Q., & Wu, Z. (2018). Recent development of boronic acid-based fluorescent sensors. RSC Advances, 8(51), 29400–29427.

(18) Bian, Z., Liu, A., Li, Y., Fang, G., Yao, Q., Zhang, G., & Wu, Z. (2020). Boronic acid sensors with double recognition sites: A review. Analyst, 145(3), 719–744.

(19) Smith, D. E., Zhang, L., & Haymet, A. D. J. (1992). Entropy of Association of Methane in Water: A New Molecular Dynamics Computer Simulation. Journal of the American Chemical Society, 114(14), 5875–5876.

(20) Chaicham, A., Sahasithiwat, S., Tuntulani, T., & Tomapatanaget, B. (2013). Highly effective discrimination of catecholamine derivatives via FRET-on/off processes induced by the intermolecular assembly with two fluorescence sensors. Chemical Communications, 49(81), 9287–9289.

(21) Hettie, K. S., & Glass, T. E. (2014). Coumarin-3-aldehyde as a scaffold for the design of tunable PET-modulated fluorescent sensors for neurotransmitters. Chemistry - A European Journal, 20(52), 17488–17499.

(22) Hettie, K. S., Liu, X., Gillis, K. D., & Glass, T. E. (2013). Fluorescent Sensor for the Visualization of Norepinephrine in Fixed. ACS Chemical Neuroscience, 4, 914–923.

(23) Martin, R., & Buchwald, S. L. (2008). Palladium-catalyzed suzuki-miyaura cross-coupling reactions employing dialkylbiaryl phosphine ligands. Accounts of Chemical Research, 41(11), 1461–1473.

(24) Barroso, S., Joksch, M., Puylaert, P., Tin, S., Bell, S. J., Donnellan, L., Duguid, S., Muir, C., Zhao, P., Farina, V., Tran, D. N., & De Vries, J. G. (2021). Improvement in the Palladium-Catalyzed Miyaura Borylation Reaction by Optimization of the Base: Scope and Mechanistic Study. Journal of Organic Chemistry, 86(1), 103–109.

(25) Lor, J. P., & Edwards, J. O. (1959). Polyol Complexes and Structure of the Benzeneboronate Ion. Journal of Organic Chemistry, 24(6), 769–774.